Supporting Information

High-performance and self-healable electromagnetic interference shielding coatings based on waterborne dynamic polyurethane and $Ti_3C_2T_x$ MXene composites

Danbee Jung,[1,2] Jae Eun Yoon,[1] Min Jun Oh,[3] Sungeun Yang,[3] Jongbum Kim,[4] Taewook Lim,[5] Taegon Oh,[1] Jungkyu Choi,[2,*] Tae Ann Kim[1,6,*]

[1]Convergence Research Center for Solutions to Electromagnetic Interference in Future-Mobility, Korea Institute of Science and Technology, Seoul 02792, Republic of Korea

[2] Department of Chemical and Biological Engineering, Korea University, Seoul 02841, Republic of Korea

[3] Center for Hydrogen Energy Materials, Korea Institute of Science and Technology, Seoul 02792, Republic of Korea

[4] Nanophotonic System Research Center, Korea Institute of Science and Technology, Seoul 02792, Republic of Korea

[5] Materials Research Team in Central Research Institute, KCC Corporation, Yongin 16891, Republic of Korea

[6] Division of Energy & Environment Technology, KIST School. Korea University of Science and Technology (UST), Seoul 02792, Republic of Korea

*Corresponding author: Prof. Jungkyu Choi (E-mail: jungkyu_choi@korea.ac.kr), Dr. Tae Ann Kim (E-mail: takim717@kist.re.kr)

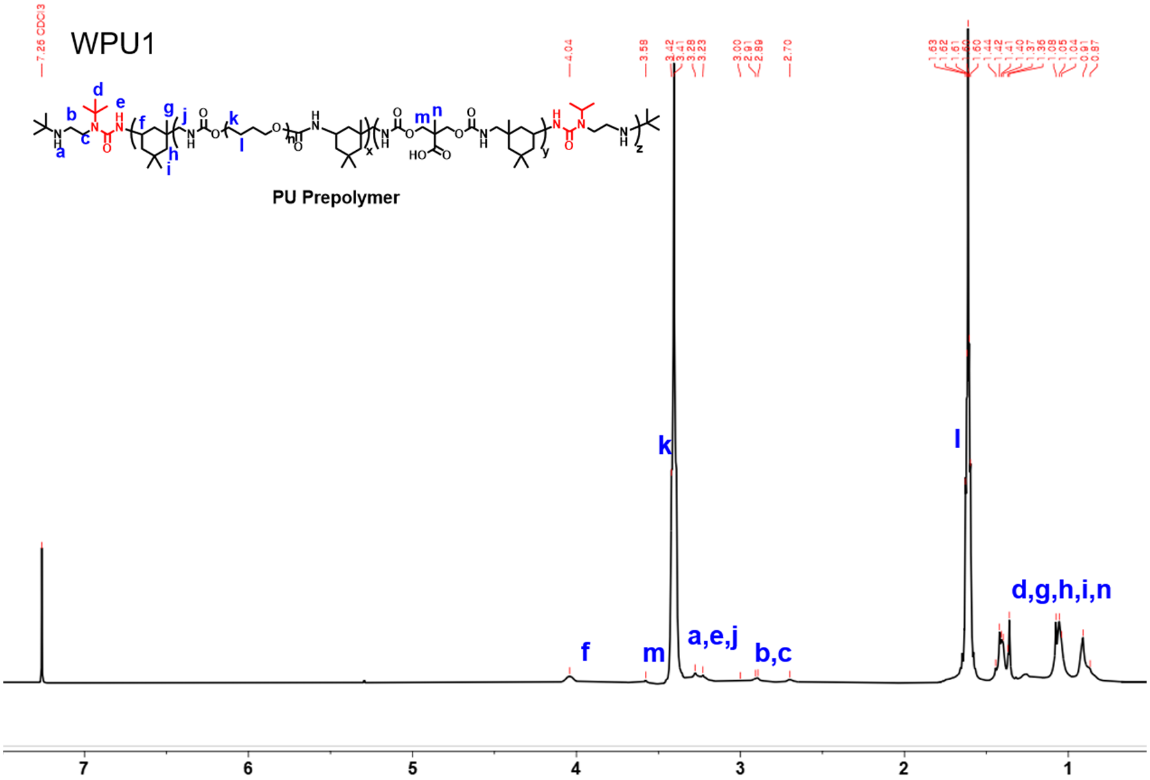

Figure S1. NMR spectra of **WPU1** prepolymer.

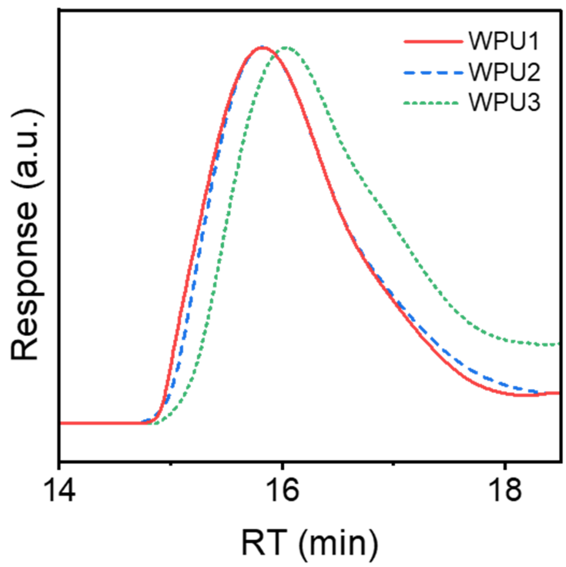

Figure S2. GPC results of WPU prepolymers.

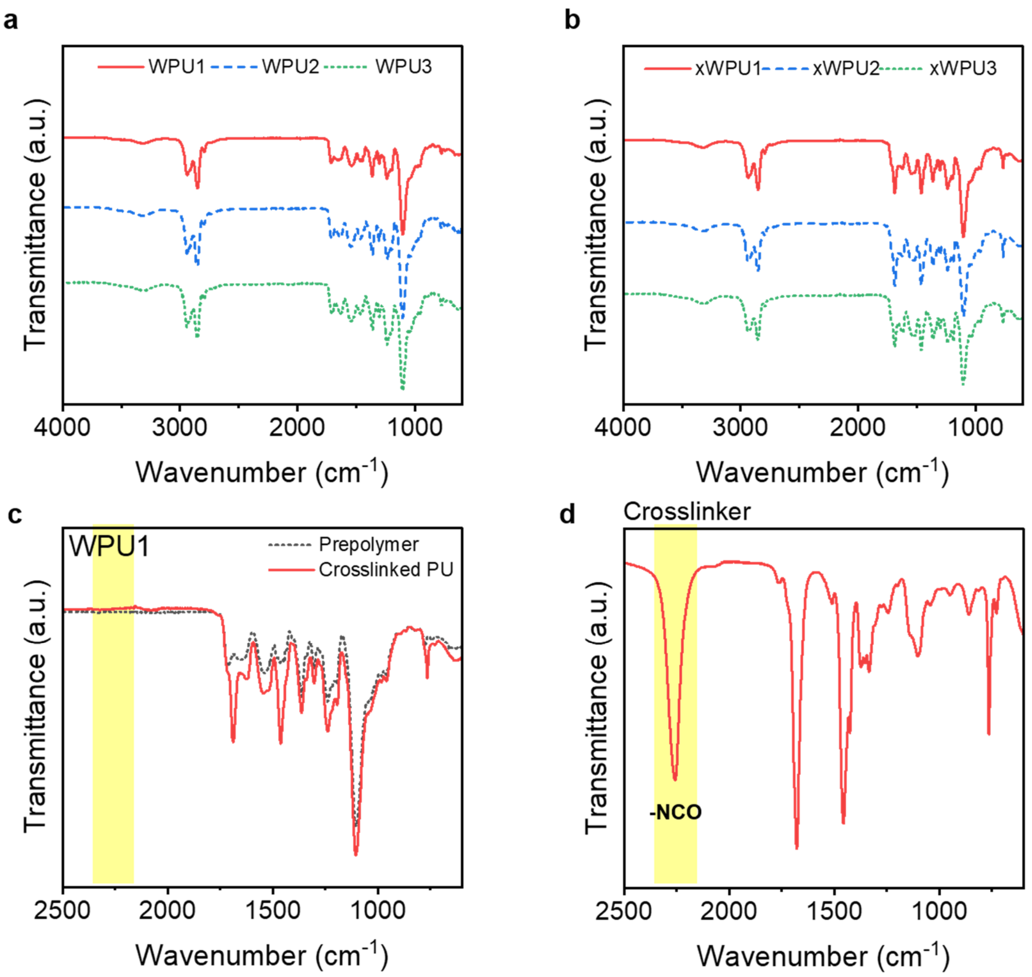

Figure S3. FT-IR spectra of (a) WPU prepolymers, (b) xWPUs, (c) **WPU1/xWPU1**, and (d). multifunctional isocyanate crosslinker.

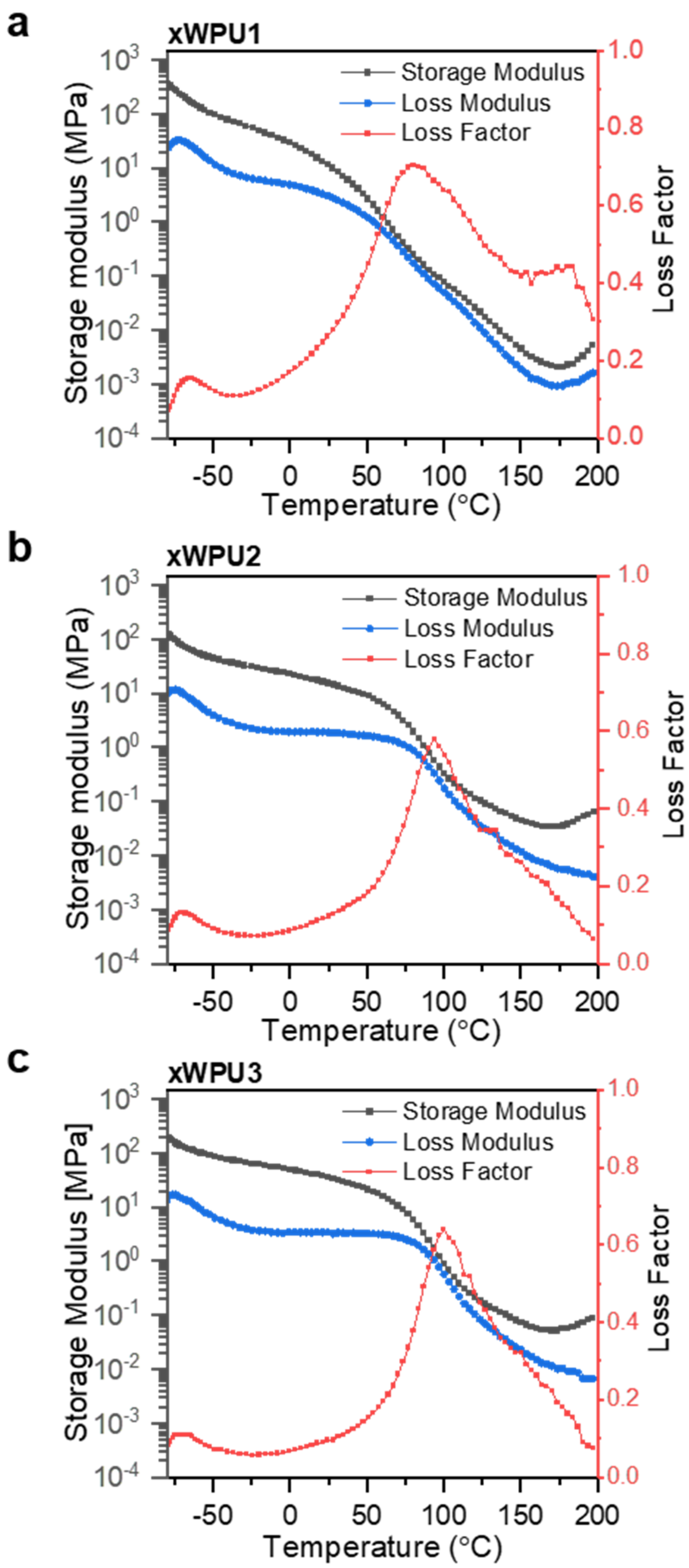

Figure S4. Temperature sweep results of (a) **xWPU1**, (b) **xWPU2**, (c) **xWPU3**.

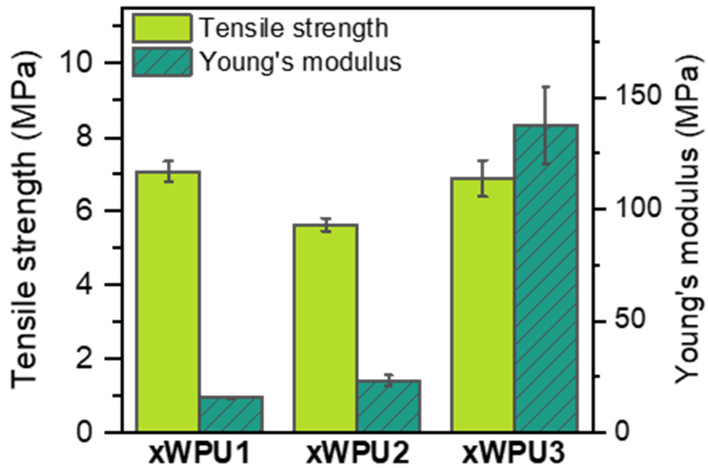

Figure S5. Tensile test results of **xWPU1**, **xWPU2**, and **xWPU3**.

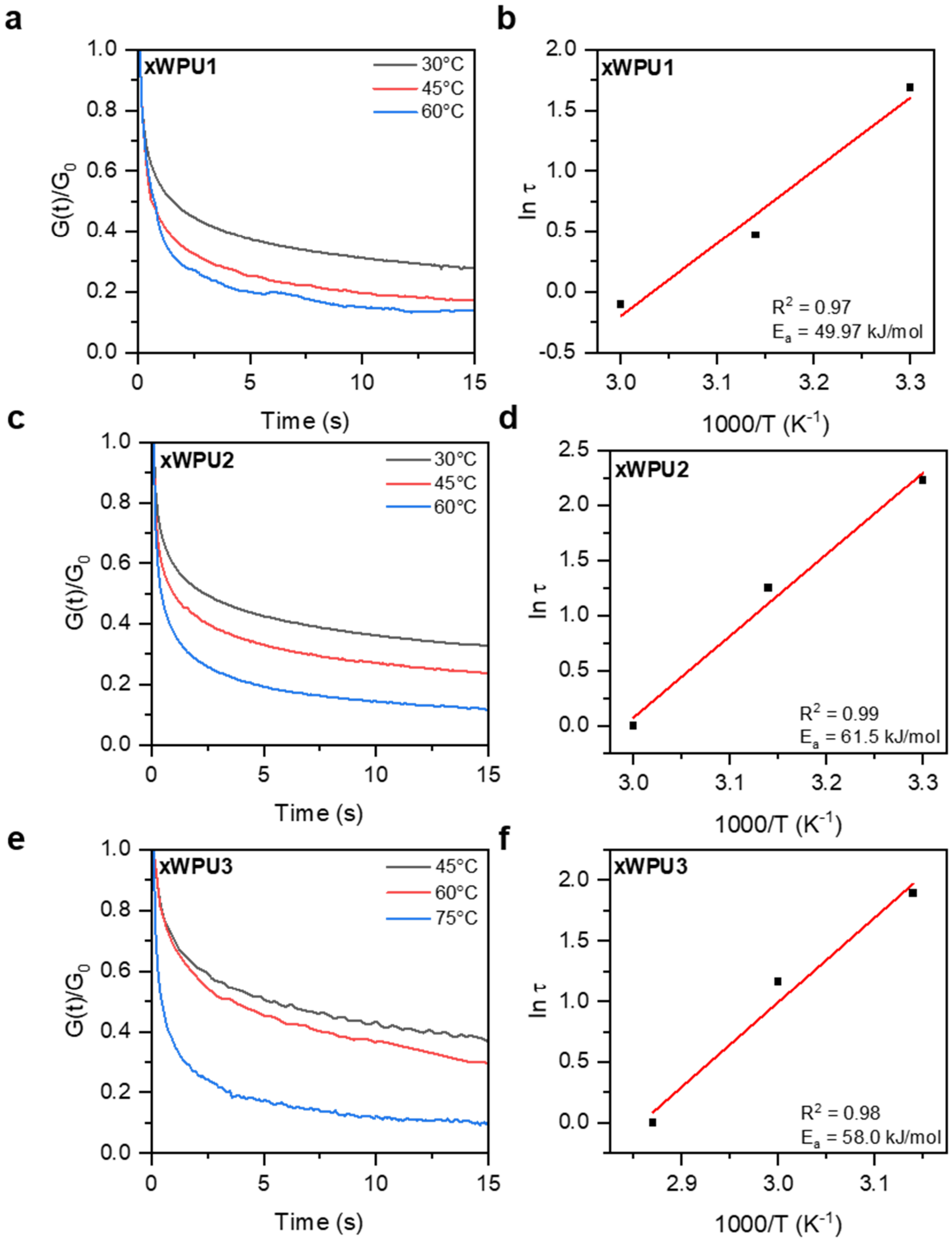

Figure S6. Stress relaxation test results of (a) **xWPU1**, (c) **xWPU2**, (d) **xWPU3** under the various temperatures. Calculation of activation energies of (b) **xWPU1**, (d) **xWPU2**, (f) **xWPU3**.

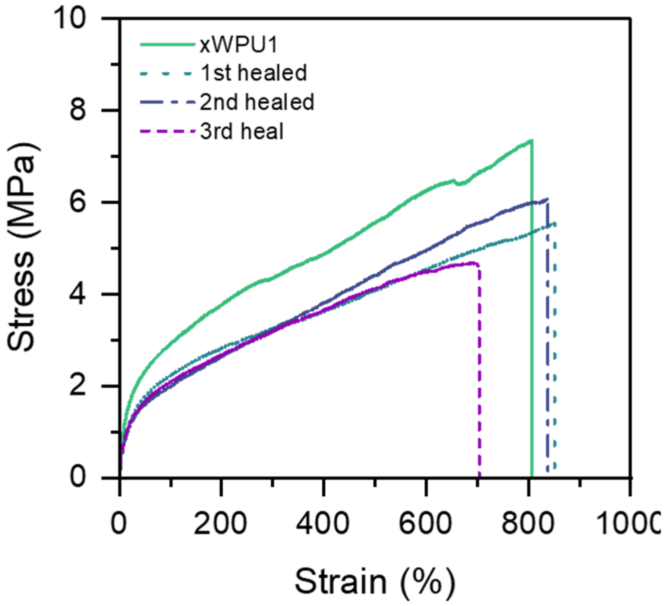

Figure S7. Stress–strain curves of the **xWPU1** composite after successive self-healing cycles.

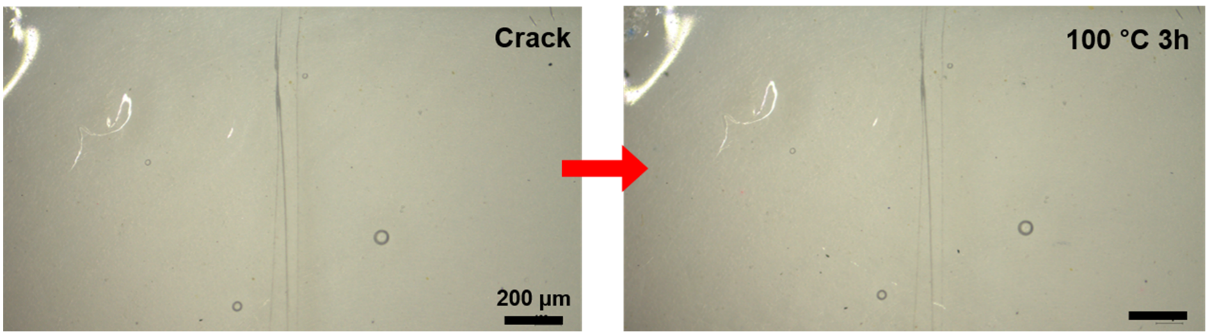

Figure S8. Self-healing test result of commercial water-dispersible polyurethane.

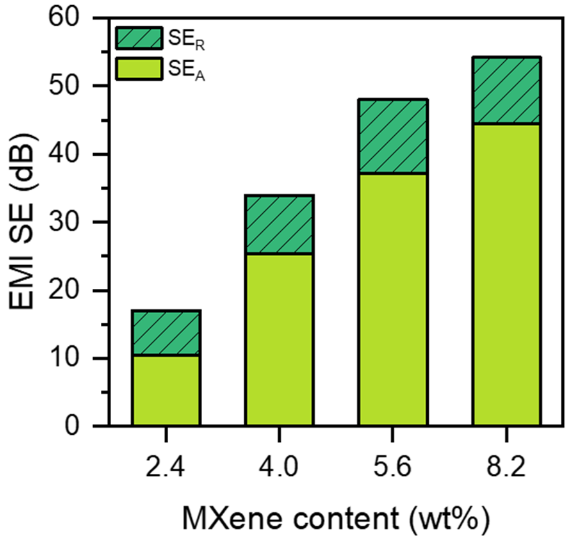

Figure S9. Absorption loss (SE_A) and reflection loss (SE_R) of MXene/**xWPU1** composites with different MXene contents.

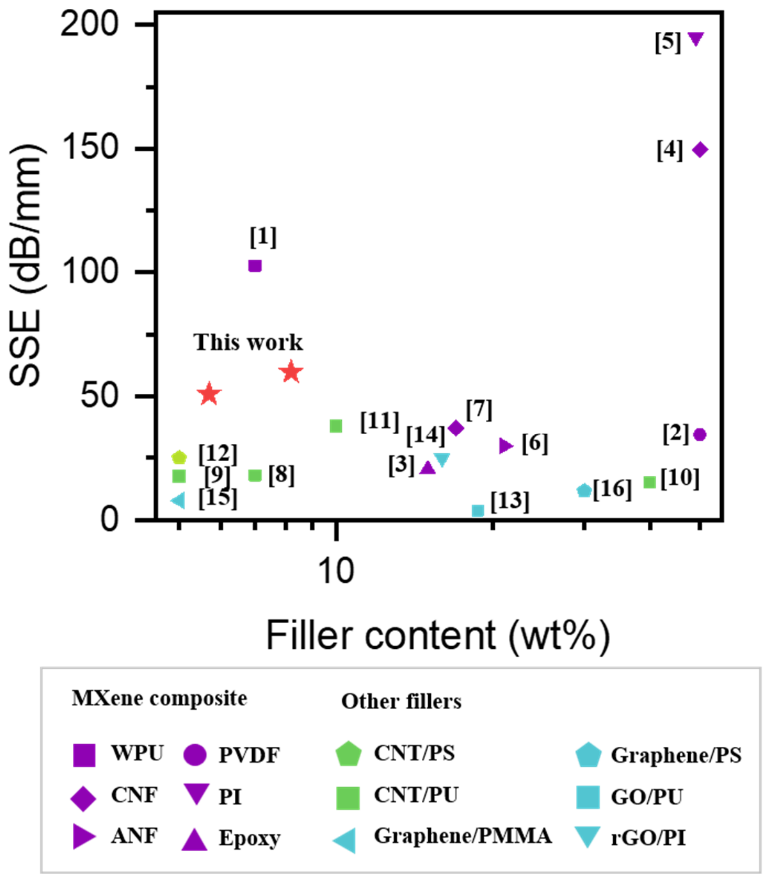

Figure S10. Comparison of EMI SE with previously reported conductive nanofiller-polymer composite materials.

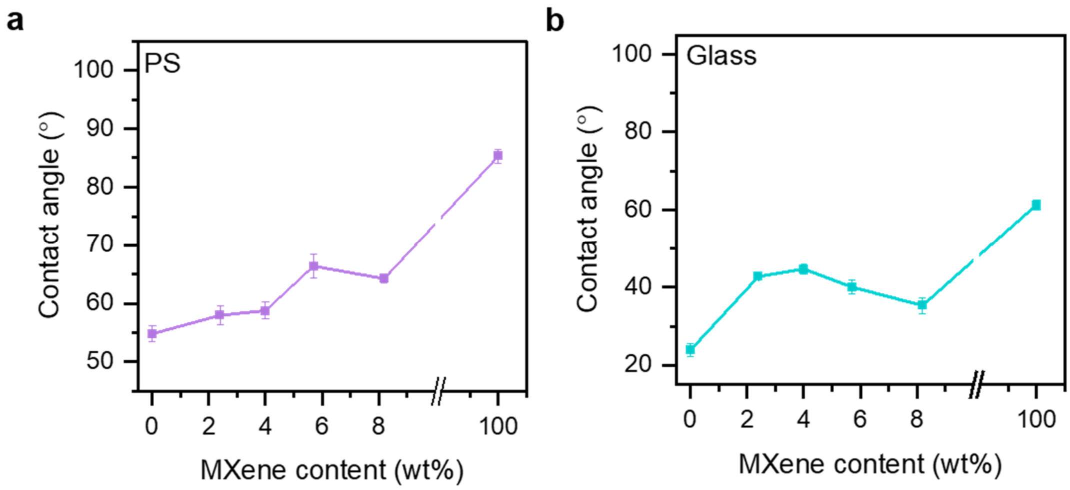

Figure S11. Change in contact angle of MXene/**xWPU1** solution on (a) PS and (b) glass

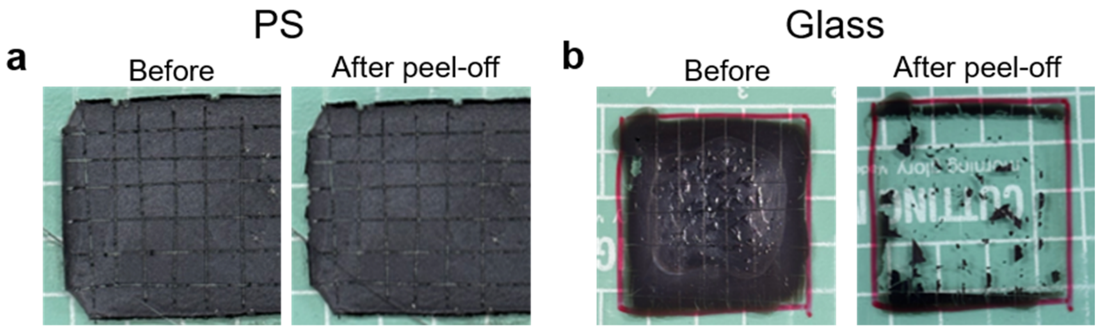

Figure S12. Peel-off test (substrate: PS, glass)

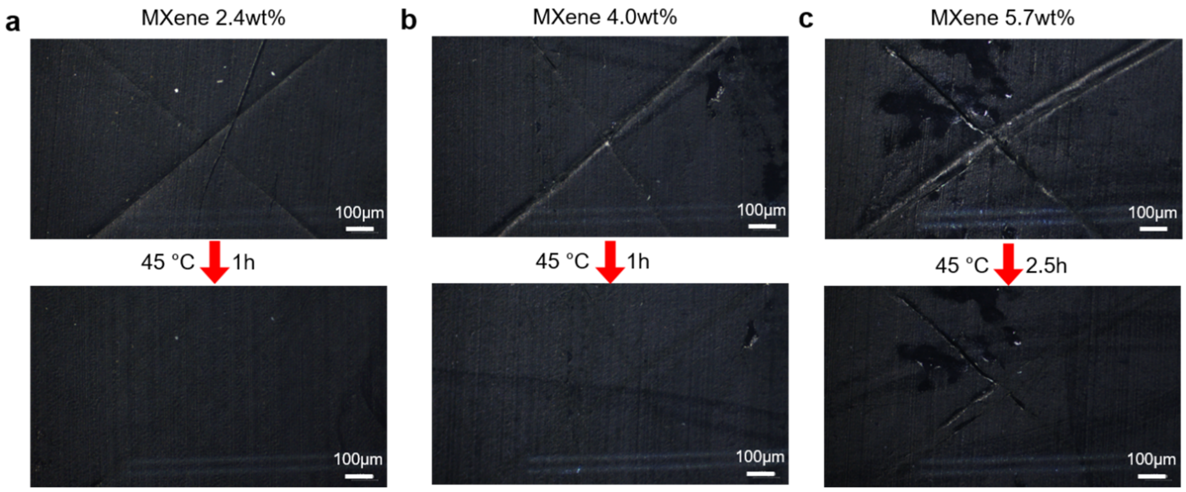

Figure S13. Thermal self-healing results of MXene/**xWPU1** composites containing (a) 2.4, (b) 4.0, (c) 5.7 wt% of MXene.

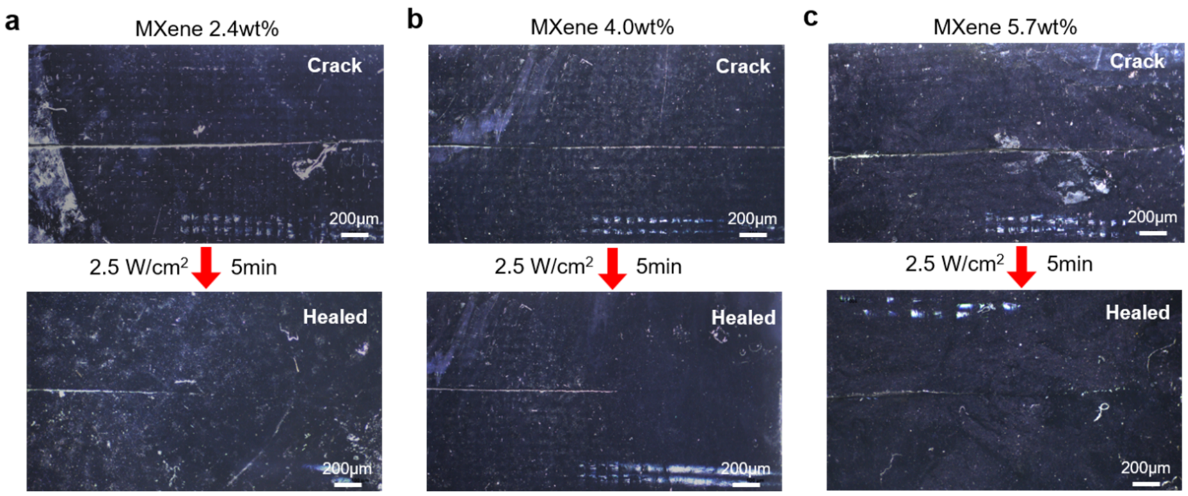

Figure S14. NIR-induced photothermal self-healing results of MXene/**xWPU1** composites containing (a) 2.4, (b) 4.0, (c) 5.7 wt% of MXene.

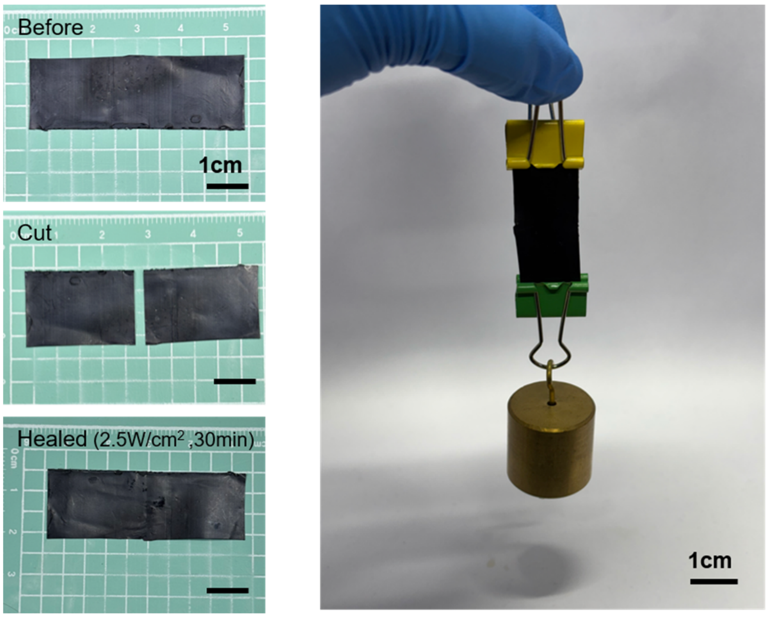

Figure S15. Macroscopic NIR-induced photothermal self-healing results of MXene/**xWPU1** composites containing.

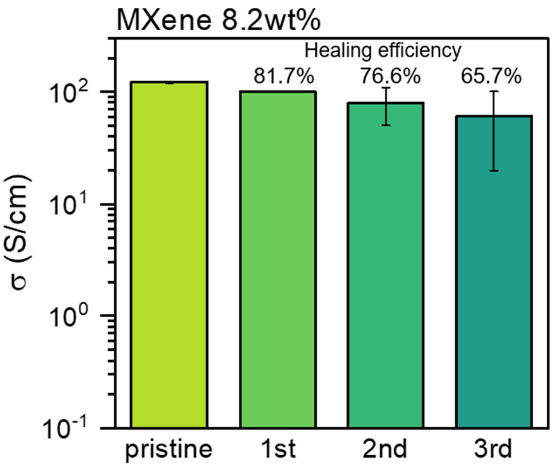

Figure S16. Electrical conductivity results after repeated thermal self-healing.

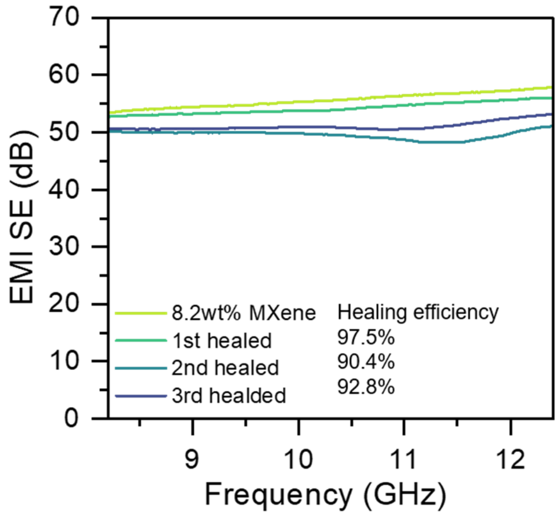

Figure S17. EMI SE results after repeated thermal self-healing.

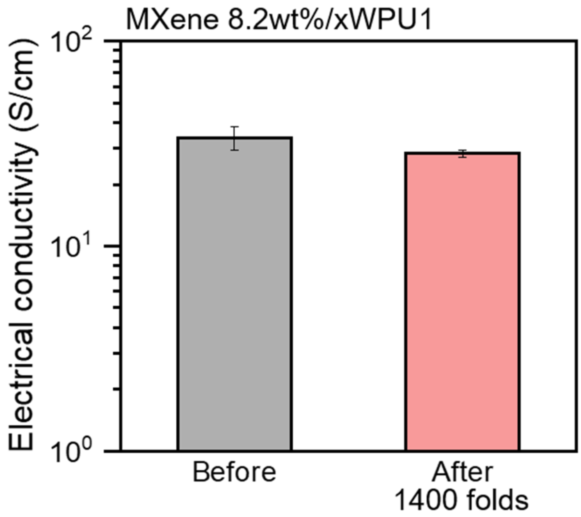

Figure S18. Electrical conductivity results of MXene and MXene 8.2wt%/**xWPU1** before and after the cyclic folding test.

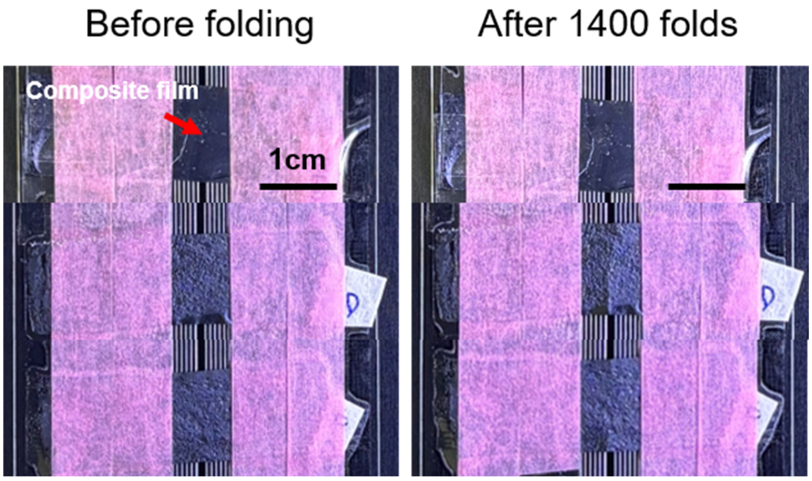

Figure S19. Digital image of MXene 8.2wt%/**xWPU1** before and after cyclic folding test.

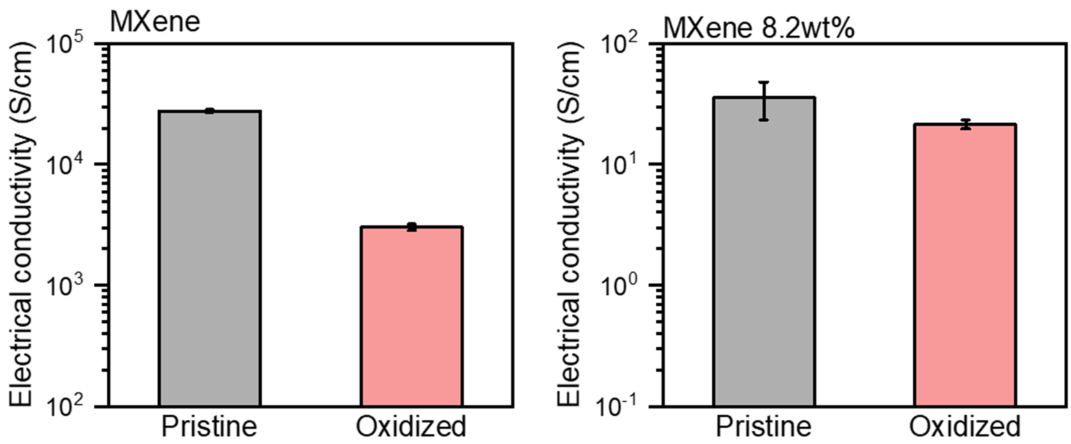

Figure S20. Electrical conductivity results of MXene and MXene 8.2wt%/**xWPU1** before and after oxidation treatment.

Table S1. Gel content values of xWPUs as a function of crosslinker content.

Crosslinker (wt%)	xWPU1	xWPU2	xWPU3
9	N/A	N/A	N/A
12	N/A	N/A	N/A
15	36.9	19.7	29.5
20	44.8	68.8	68.4
30	57.0	-	86.1
40	-	66.6	85.0

Table S2. Power coefficients (reflection, transmission, and absorption) of MXene/**xWPU1** composites with different MXene contents.

MXene content (wt%)	Reflection	Transmittance	Absorption
2.4	0.778	0.0213	0.201
4.0	0.856	5.10×10^{-4}	0.143
5.6	0.912	2.00×10^{-5}	0.088
8.2	0.890	3.98×10^{-6}	0.110

Table S3. The comparison of MXene/**xWPU1** and other conductive nanofiller/polymer composites for EMI shielding.

Entry	Filler	Matrix	Filler content (wt%)	EMI SE/t (dB/mm)	Ref.
1	MXene	WPU	7	103	[1]
2	MXene	PVDF	50	34.5	[2]
3	MXene	Epoxy	15	20.5	[3]
4	MXene	CNF	50	150	[4]
5	MXene	PI	49	195	[5]
6	MXene	ANF	21	29.9	[6]
7	MXene	CNF	17	37.3	[7]
8	CNT	PU	7	18.0	[8]
9	CNT	PU	5	17.5	[9]
10	PCNT	PU	40	15.3	[10]
11	CNT	TPU	10	38.1	[11]
12	CNT	PS	5	25.0	[12]
13	GO	PU	19	3.89	[13]
14	rGO	PI	16	25.0	[14]
15	Graphene	PMMA	5	7.90	[15]
16	Graphene	PS	30	11.7	[16]
17	MXene	WPU	5.7	51.0	This work
18			8.2	59.8	

Table S4. Tensile test results of MXene/**xWPU1** composites.

	Young's Modulus (MPa)	Tensile Strength (MPa)	Elongation at Break (%)
xWPU1	15.9 ± 0.45	7.08 ± 0.28	842 ± 36
MXene 2.4wt%	21.8 ± 0.35	8.35 ± 0.15	797± 11
MXene 4.0wt%	26.1 ± 4.0	11.6 ± 0.35	1280 ± 6.5
MXene 5.7wt%	38.7 ± 2.2	12.5 ± 0.38	889 ± 130
MXene 8.2wt%	69.1 ± 4.6	11.0 ± 1.1	775 ± 90

References

1. Lu J, Zhang Y, Tao Y, Wang B, Cheng W, Jie G, Song L, Hu Y (2021) Self-healable castor oil-based waterborne polyurethane/MXene film with outstanding electromagnetic interference shielding effectiveness and excellent shape memory performance. J Colloid Interface Sci 588:164–174. https://doi.org/10.1016/j.jcis.2020.12.076

2. Rajavel K, Luo S, Wan Y, Yu X, Hu Y, Zhu P, Sun R, Wong C (2020) 2D Ti3C2Tx MXene/polyvinylidene fluoride (PVDF) nanocomposites for attenuation of electromagnetic radiation with excellent heat dissipation. Compos Part A Appl Sci Manuf 129:. https://doi.org/10.1016/j.compositesa.2019.105693

3. Wang L, Chen L, Song P, Liang C, Lu Y, Qiu H, Zhang Y, Kong J, Gu J (2019) Fabrication on the annealed Ti3C2Tx MXene/Epoxy nanocomposites for electromagnetic interference shielding application. Compos B Eng 171:111–118. https://doi.org/10.1016/j.compositesb.2019.04.050

4. Cao WT, Chen FF, Zhu YJ, Zhang YG, Jiang YY, Ma MG, Chen F (2018) Binary Strengthening and Toughening of MXene/Cellulose Nanofiber Composite Paper with Nacre-Inspired Structure and Superior Electromagnetic Interference Shielding Properties. ACS Nano 12:4583–4593. https://doi.org/10.1021/acsnano.8b00997

5. Sun K, Wang F, Yang W, Liu H, Pan C, Guo Z, Liu C, Shen C (2021) Flexible Conductive Polyimide Fiber/MXene Composite Film for Electromagnetic Interference Shielding and Joule Heating with Excellent Harsh Environment Tolerance. ACS Appl Mater Interfaces 13:50368–50380. https://doi.org/10.1021/acsami.1c15467

6. Lu Z, Jia F, Zhuo L, Ning D, Gao K, Xie F (2021) Micro-porous MXene/Aramid nanofibers hybrid aerogel with reversible compression and efficient EMI shielding performance. Compos B Eng 217:. https://doi.org/10.1016/j.compositesb.2021.108853

7. Zeng Z, Wang C, Siqueira G, Han D, Huch A, Abdolhosseinzadeh S, Heier J, Nüesch F, Zhang C, Nyström G (2020) Nanocellulose-MXene Biomimetic Aerogels with Orientation-Tunable Electromagnetic Interference Shielding Performance. Advanced Science 7:. https://doi.org/10.1002/advs.202000979

8. Wang T, Yu WC, Zhou CG, Sun WJ, Zhang YP, Jia LC, Gao JF, Dai K, Yan DX, Li ZM (2020) Self-healing and flexible carbon nanotube/polyurethane composite for efficient electromagnetic interference shielding. Compos B Eng 193:. https://doi.org/10.1016/j.compositesb.2020.108015

9. Feng D, Xu D, Wang Q, Liu P (2019) Highly stretchable electromagnetic interference (EMI) shielding segregated polyurethane/carbon nanotube composites fabricated by microwave selective sintering. J Mater Chem C Mater 7:7938–7946. https://doi.org/10.1039/c9tc02311a

10. Gahlout P, Choudhary V (2020) EMI shielding response of polypyrrole-MWCNT/polyurethane composites. Synth Met 266:.

https://doi.org/10.1016/j.synthmet.2020.116414

11. Shin B, Mondal S, Lee M, Kim S, Huh Y Il, Nah C (2021) Flexible thermoplastic polyurethane-carbon nanotube composites for electromagnetic interference shielding and thermal management. Chemical Engineering Journal 418:. https://doi.org/10.1016/j.cej.2021.129282
12. Yang Y, Gupta MC, Dudley KL, Lawrence RW (2005) A comparative study of EMI shielding properties of carbon nanofiber and multi-walled carbon nanotube filled polymer composites. J Nanosci Nanotechnol 5:927–931. https://doi.org/10.1166/jnn.2005.115
13. Hu Z, Ji X, Li B, Luo Y (2019) A self-assembled graphene/polyurethane sponge for excellent electromagnetic interference shielding performance. RSC Adv 9:25829–25835. https://doi.org/10.1039/c9ra02059d
14. Li Y, Pei X, Shen B, Zhai W, Zhang L, Zheng W (2015) Polyimide/graphene composite foam sheets with ultrahigh thermostability for electromagnetic interference shielding. RSC Adv 5:24342–24351. https://doi.org/10.1039/c4ra16421k
15. Zhang H Bin, Yan Q, Zheng WG, He Z, Yu ZZ (2011) Tough graphene-polymer microcellular foams for electromagnetic interference shielding. ACS Appl Mater Interfaces 3:918–924. https://doi.org/10.1021/am200021v
16. Yan DX, Ren PG, Pang H, Fu Q, Yang MB, Li ZM (2012) Efficient electromagnetic interference shielding of lightweight graphene/polystyrene composite. J Mater Chem 22:18772–18774. https://doi.org/10.1039/c2jm32692b